In-phase antiguided bottom-emitting vertical cavity laser arrays

M.T. Johnson, D.F. Siriani, P.O. Leisher and K.D. Choquette

In-phase emission from a bottom-emitting, coherently coupled, vertical cavity surface-emitting laser array is demonstrated for the first time. Various array geometries are examined. An antiguided index profile is used to obtain the preferred on-axis far-field peak from a 2 × 1 array up to 0.9 mW, representing a critical step towards coherent, high-brightness two-dimensional laser arrays.

Introduction: Two-dimensional (2D)-phased vertical cavity surface-emitting laser (VCSEL) arrays offer unique advantages for scaling up single-mode power for high-brightness applications such as fibre laser pumps. They tend, however, to operate in the undesirable out-of-phase mode, which has an on-axis null in the far field [1]. In-phase VCSEL arrays with an on-axis maximum in the far field have been obtained primarily with antiguided, top-emitting designs [2–5]. These structures, however, face difficult challenges in thermal management and current injection uniformity, especially for larger arrays. These difficulties can be substantially mitigated with a bottom-emitting design, as commonly used for high-power incoherent 2D VCSEL arrays. The key design advantages include significantly reducing thermal resistance from the active region to the heatsink and direct current injection into the array elements. Previous bottom-emitting coherent arrays have employed reflectivity modulation and/or mesa etching, which led to an out-of-phase operation [1, 6, 7]. We report a bottom-emitting VCSEL array with an antiguided index profile created by a simple, self-aligned process to demonstrate in-phase, continuous-wave (CW) emission, which represents a critical step towards coherent, high-brightness arrays.

Fabrication: The bottom-emitting arrays, as shown in the schematic of Fig. 1, consist of an *n*-doped GaAs substrate, a 29-period n-type output distributed Bragg reflector (DBR), an active region emitting nominally at 980 nm and a high reflectivity p-type DBR with 30 periods. An array of 6 × 6 µm, 3 µm-thick Au squares are formed by an electroplating process (over a thin Au layer) to define both the ohmic contact and an ion implantation mask to pixelate current injection into the array elements [4]. After thinning the substrate, an electrode pattern was deposited on the polished substrate side around the array perimeter. The array size is determined in this work by patterns etched with a focused ion beam into the high reflectivity DBR. The current injected into the elements creates an antiguided index pattern which can support the 'in-phase' mode, where neighbouring elements are locked in phase [8].

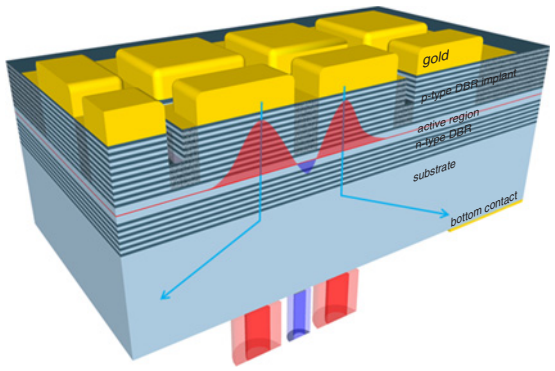

Fig. 1 *Bottom-emitting 2D VCSEL array structure*

Single VCSEL emitter: The CW light and voltage against current curves for a single-element bottom emitter with a 5 µm diameter are shown in Fig. 2. The laser output shows an oscillating behaviour that stems from the interference effects of the substrate/air interface. The far-field profiles of Fig. 2*a* are also found to vary with the cyclic interference effects, while the spectra in Fig. 2*b* show single-mode behaviour through rollover. The far-field full width at half maximum (FWHM) for this single element is found to be 5.4°.

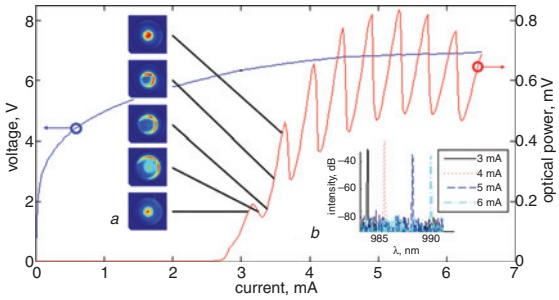

Fig. 2 *Output characteristics for single, 5 µm diameter VCSEL*
a Far-field profiles at varying current injection
b Single-mode spectra at varying current injection

2 × 1 VCSEL array: Near-field images of a 2 × 1 array operating below threshold and at 8.7 mA ($1.3 \times I_{threshold}$) with 0.9 mW output power are shown in Figs. 3*a* and *b*, respectively. The sub-threshold image reveals the carrier density distribution caused by the ion-implantation apertures. A slice of the near field is taken at the black line in Fig. 3*a* to estimate the refractive index profile. This profile is shown in Fig. 3*c* and is determined from the same maximum carrier density value (5×10^{18} cm^{-3}) and temperature distribution described in [8]. Given this index profile, a one-dimensional Helmholtz equation is solved using the finite difference method to yield the theoretical near-field modal intensity shown in Fig. 3*c* [8]. The measured near-field slice from Fig. 3*b* is also displayed for comparison in Fig. 3*c* and shows good agreement, including the fringe between the elements.

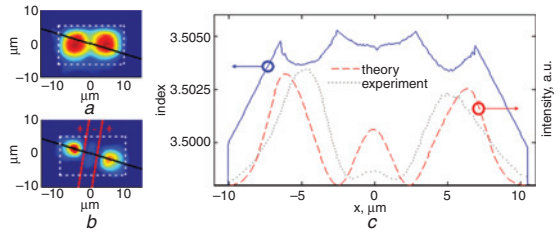

Fig. 3 *Near-field intensities and refractive index for 2 × 1 array*
a Sub-threshold near-field image with dashed border
b Near field operating in [+/+] mode at current of 8.7 mA
c Refractive index and theoretical and experimental near-field modal profiles obtained along black lines shown in Figs. *a* and *b*

On separating the near field into the three elements delineated by the red lines shown in Fig. 3*b*, the left and right elements labelled '+' are assumed to be in-phase, whereas the central lobe labelled '−' is assumed to be π out-of-phase. The beam is then propagated to the far field based on the Fraunhofer approximation [9]. This simulated far field, displayed in Fig. 4*a*, shows good agreement with the experimentally determined far field shown in Fig. 4*b*, which has a FWHM of 2.1°. The lasing spectra, plotted at various currents in Fig. 4*c*, show that the array operates in a single mode under an injection current range of 8.7 ± 0.5 mA. Our observations thus demonstrate that the array is operating in the preferred [+/+] mode with an on-axis far-field maximum.

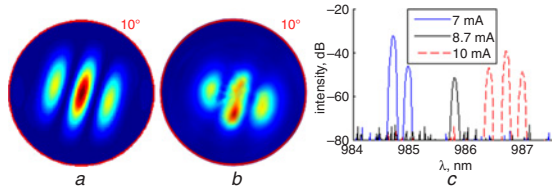

Fig. 4 *Far-field intensities and spectral data for 2 × 1 array*
a Simulated far field as propagated from Fig. 3*b*
b Far field with injection current of 8.7 mA
c Spectra showing single-mode operation with injection current of 8.7 mA

2D VCSEL arrays: Intensity profiles for 2D bottom-emitting arrays are depicted in Fig. 5. A sub-threshold near-field image for a 2 × 2 array is shown in Fig. 5*b*, indicating gain pixelation. The far field at 6.4 mA ($1.3 \times I_{threshold}$) current injection is shown in Fig. 5*a*, and exhibits a

narrow on-axis lobe as expected for a 2D in-phase array [5]. However, the corresponding near-field image in Fig. 5*c* and the multimode spectral data do not correlate with a single in-phase mode. The FWHM of the central far-field lobe in Fig. 5*a* is 3.8°, which is between that mentioned above for the single element and the in-phase 2 × 1 array, indicating partial coherence.

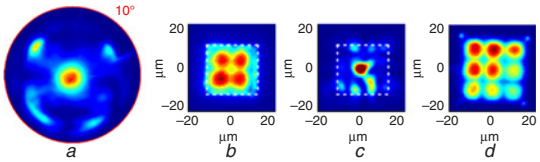

Fig. 5 *Near- and far-field intensities from 2 × 2 and 3 × 3 arrays*

a Far field of 2 × 2 array at injection current of 6.4 mA
b Sub-threshold near-field image of 2 × 2 array with dashed border
c Near-field image of 2 × 2 array at injection current of 6.4 mA
d Sub-threshold near-field image of 3 × 3 array

It is difficult to achieve uniform current injection in top-emitting arrays with more than two elements in both dimensions. One approach is to use metal contacts between the array elements, but unless carefully phase matched [3], this has the undesired effect of discriminating against the preferred in-phase mode [1, 6]. The sub-threshold image of a 3 × 3 bottom-emitting array is shown in Fig. 5*d*. The current is found to distribute much more evenly than that which is observed with top-emitting arrays. Above threshold, this 3 × 3 array was found to support multiple modes simultaneously because of lack of sufficient modal discrimination.

Conclusions: Various ion-implanted bottom-emitting VCSEL array geometries have been characterised. We have demonstrated the first in-phase operation of a coherently coupled bottom-emitting VCSEL array and shown improved current uniformity in a large array, representing a critical step towards coherent, high-brightness, 2D VCSEL arrays. The primary challenges encountered are interference effects and lack of sufficient modal discrimination. Optical interference arising from the substrate/air interface can be mitigated by deposition of an anti-reflection coating onto the substrate. Improved modal discrimination requires careful design and control of the real and imaginary parts of the array's index profile. Some approaches to achieve this include varying the element size and separations, incorporating a photonic crystal pattern [5, 8], and patterning the top metal to vary the reflectivity profile [1, 3].

3 June 2013
doi: 10.1049/el.2013.1867
One or more of the Figures in this Letter are available in colour online.

M.T. Johnson, D.F. Siriani, P.O. Leisher and K.D. Choquette (*Department of Electrical and Computer Engineering, University of Illinois, Urbana, IL 61801, USA*)

E-mail: mtjohns2@illinois.edu

D.F. Siriani: Now with the MIT Lincoln Laboratory, Lexington, MA 02420, USA

P.O. Leisher: Now with the Department of Physics and Optical Engineering, Rose-Hulman Institute of Technology, Terre Haute, IN 47803, USA

References

1 Orenstein, M., Kapon, E., Harbison, J., Florez, L., and Stoffel, N.: 'Large two-dimensional arrays of phase-locked vertical cavity surface emitting lasers', *Appl. Phys. Lett.*, 1992, **60**, (13), pp. 1535–1537
2 Serkland, D.K., Choquette, K., Hadley, G., Geib, K., and Allerman, A.: 'Two-element phased array of antiguided vertical-cavity lasers', *Appl. Phys. Lett.*, 1999, **75**, (24), pp. 3754–3756
3 Bao, L., Kim, N.H., Mawst, L.J., Elkin, N.N., Troshchieva, V.N., Vysotsky, D.V., and Napartovich, A.P.: 'Near-diffraction-limited coherent emission from large aperture antiguided vertical-cavity surface-emitting laser arrays', *Appl. Phys. Lett.*, 2004, **84**, (3), pp. 320–322
4 Lehman, A.C., and Choquette, K.D.: 'One- and two-dimensional coherently coupled implant defined vertical cavity laser arrays', *IEEE Photonics Technol. Lett.*, 2007, **19**, (19), pp. 1421–1423
5 Siriani, D.F., and Choquette, K.D.: 'In-phase, coherent photonic crystal vertical-cavity surface-emitting laser arrays with low divergence', *Electron. Lett.*, 2010, **46**, (10), pp. 712–714
6 Morgan, R.A., Kojima, K., Mullally, T., Guth, G.D., Focht, M.W., Leibenguth, R.E., and Asom, M.: 'High-power coherently coupled 8 × 8 vertical cavity surface emitting laser array', *Appl. Phys. Lett.*, 1992, **61**, (10), pp. 1160–1162
7 Yoo, H.J., Hayes, J.R., Paek, E.G., Harbison, J.P., Florez, L.T., and Kwon, Y.S.: 'Phase-locked two-dimensional arrays of implant isolated vertical cavity surface emitting lasers', *Electron. Lett.*, 1990, **26**, (23), pp. 1944–1946
8 Siriani, D.F., and Choquette, K.D.: 'Implant defined anti-guided vertical-cavity surface-emitting laser arrays', *IEEE J. Quantum Electron.*, 2011, **47**, (2), pp. 160–164
9 Johnson, M.T., Siriani, D.F., Sulkin, J.D., and Choquette, K.D.: 'Phase and coherence extraction from a phased vertical cavity laser array', *Appl. Phys. Lett.*, 2012, **101**, (3), pp. 031116–031116-4